OXFORD

Research Article

Obesity alters phosphoramide mustard-induced ovarian DNA repair in mice[†]

Shanthi Ganesan, Jackson Nteeba, Jill A. Madden and Aileen F. Keating[*]

Department of Animal Science, Iowa State University, Ames, Iowa, USA

[*]Correspondence: Department of Animal Science, Iowa State University, Ames, IA 50011, USA. Tel: +1-515-294-3849;
Fax: +1-515-294-4471; E-mail: akeating@iastate.edu

Abstract

Phosphoramide mustard (PM) destroys rapidly dividing cells and activates the DNA double strand break marker, γH2AX, and DNA repair in rat granulosa cells and neonatal ovaries. The effects of PM exposure on DNA damage and activation of DNA damage repair in lean and obese female mice were investigated. Wild type (lean) non agouti (a/a) and KK.Cg-Ay/J heterozygote (obese) mice received sesame oil or PM (95%; 25 mg/kg; intraperitoneal injection). Obesity increased ($P <$ 0.05) hepatic and spleen but decreased ($P <$ 0.05) uterine weight. PM exposure reduced ($P <$ 0.05) spleen weight regardless of body composition, however, decreased ($P <$ 0.05) ovarian and hepatic weight were observed in the obese PM-exposed females. PM decreased ($P <$ 0.05) primordial and primary follicle number in lean females. Obesity and PM increased ($P <$ 0.05) γH2AX protein. DNA damage repair genes *Prkdc*, *Parp1*, and *Rad51* mRNA were unaltered by obesity, however, *Atm* and *Xrcc6* mRNA were increased ($P <$ 0.05) while *Brca1* was reduced ($P <$ 0.05). Obesity reduced ($P <$ 0.05) PRKDC, XRCC6 and but increased ($P <$ 0.05) ATM protein. ATM, BRCA1 and RAD51 protein levels were increased ($P <$ 0.05) by PM exposure in both lean and obese mice, while PM-induced increased ($P <$ 0.05) XRCC6 and PARP1 were observed only in lean mice. Thus, PM induces ovarian DNA damage *in vivo*; obesity alters DNA repair response gene mRNA and protein level; the ovary activates DNA repair proteins in response to PM; but obesity compromises the ovarian PM response.

Summary Sentence

PM exposure induces DNA damage and subsequent repair in ovaries of exposed mice, and this response is abrogated in obese females.

Key words: ovary, PM, ovotoxicity, DNA double strand breaks repair, obesity.

Abbreviations

BRCA1   breast cancer 1, early onset
BRCA2   breast cancer 2, early onset
ATR   ataxia telangiectasia and Rad3 related
Prkdc   protein kinase, DNA activated, catalytic polypeptide
Parp1   poly (ADP-ribose) polymerase family, member 1
Rad51   RAD51 recombinase

Xrcc6   X-ray repair complementing defective repair in Chinese hamster cells 6
Gapdh   glyceraldehyde-3-phosphate dehydrogenase

Introduction

The mammalian ovary is the female gamete-producing reproductive organ. Primordial germ cells undergo mitosis during oogenesis to

establish a gamete pool, arrested in the diplotene stage of meiosis [1]. Females are born with a finite number of gametes, contained in primordial follicle structures, which are required to remain viable over the female reproductive lifetime [1]. Primordial follicles are activated to either develop towards ovulation or undergo atresia, a natural process of elimination [2]. Through this process, females are eventually depleted of all follicles and reproductive senescence ensues [1,2]. Several factors, including genetics and ovotoxic chemical exposures, accelerate loss of follicles [3,4], which can phenotypically manifest as infertility and premature ovarian failure.

Cyclophosphamide (CPA) is a chemotherapeutic agent used to treat cancer and autoimmune diseases. Cyclophosphamide can induce rapid amenorrhea, potentially due to antral follicle destruction, or premature ovarian failure, attributed to primordial follicle depletion [5]. Cyclophosphamide has also been demonstrated to cause infertility by increasing the number of early growing follicles and decreasing primordial follicle numbers through follicular activation in mice ovaries [6], a phenomenon previously observed in ovotoxicity induced by 4-vinylcyclohexene diepoxide [7]. In rodents, species-specific differences in CPA-induced ovarian toxicity is noted, with primordial follicles being most sensitive in mice [8] and antral follicles in rats [9]. Oxidation of CPA by hepatic cytochromes p450 2B1 and 3A4 to 4-hydroxycyclophosphamide (4-OH-CPA) leads to a cascade of nonenzymatic reactions and ultimately culminating in the production of phosphoramide mustard (PM) [10]. Phosphoramide mustard has been shown to be an active ovotoxic CPA metabolite by destroying both primordial and primary follicles [8,11,12]. Phosphoramide mustard-induced DNA damage is at least one mechanism by which ovarian follicle loss is caused [13–15]. Phosphoramide mustard is known to destroy rapidly dividing cells by covalently binding to DNA, inducing DNA–DNA, DNA–protein cross links, and DNA double strand breaks (DSBs) [16–18]. Upon DSB induction, cells activate their DNA damage response (DDR) that comprises cell cycle arrest, DNA damage repair, and subsequent cell cycle resumption [19–22]. Phosphorylation of the histone H2AX (γH2AX) at Serine 19 is an early event in the DDR, resulting in recruitment and maintenance of DNA repair molecules at the sites of DSB until repair is complete, and is considered a gold standard for DSB localization. γH2AX can be activated by ataxia-telangiectasia mutated (ATM), ATM-related (ATR), and DNA-dependent protein kinases in response to DSB. Repair of the break can be accomplished through the action of two major pathways: nonhomologous end joining (NHEJ) and homologous recombination (HR). The integrity of the gamete genome is critical for the health of offspring. If alterations in DNA of primordial follicles remain, these changes could cause detrimental changes in offspring as evidenced in mice exposed once to CPA who displayed increased malformations [23]. This is therefore a major concern for women wishing to have children subsequent to cancer treatments [24].

Obesity induces DNA damage in hematopoietic cell transplant recipients that have been treated by CPA [25]. It is known that cellular DNA damage can arise from the action of free radicals and obesity [26]. In addition, high-fat diets can accelerate oxidative stress and oxidative DNA damage [27]. BRCA1 and BRCA2 are crucial members of the ATM-mediated DSB repair family of genes. Impairment of BRCA1-related DNA DSB repair was associated with accelerated loss of the ovarian follicular reserve and with accumulation of DSB in human oocytes, suggesting that DNA DSB repair efficiency is an important determinant of oocyte aging in women [28]. Obesity affects approximately 30% of US adults, and adverse effects of obesity on reproductive health have been documented, and include reduced

conception and implantation [29,30], impaired fecundity [30–33], and infertility [29,34]. Obese mothers have increased risk for miscarriage [35], poor oocyte quality [36], and birth defects in their offspring [35]. It is also recognized that increased body mass index is a risk factor for ovarian cancer [37]. Mortality rates from ovarian cancer are greater in overweight and obese, relative to lean, women [38]. Furthermore, although studies are limited, a recent report positively associated human offspring cancer incidence with maternal obesity [39].

Our previous studies have indicated the presence of DNA damage at a basal level in the ovaries of obese mice, and demonstrated increased sensitivity to another ovotoxicant 7,12-dimethylbenz[a]anthracene (DMBA) [40], which similar to PM is an alkylating agent. Also, our work using cultured ovarian granulosa cells [14] and an ex vivo ovarian culture system [15] demonstrated PM-induced DNA damage as a mode of ovotoxicity. Thus, we hypothesized that PM-induced ovotoxicity would cause DNA DSBs in vivo, to which the ovary will mount a protective DNA repair response. In addition, we proposed that the ovaries of obese mice would have an altered response to PM exposure. Moreover, we hypothesized that an interaction between PM exposure and obesity would exist.

Methods and materials

Reagents

Phosphoramide mustard was acquired from the National Institutes of Health National Cancer Institute (Bethesda, MA). Sesame oil (SO) (CAS # 8008-74-0), 2-β-mercaptoethanol, 30% acrylamide/0.8% bisacrylamide, ammonium persulphate, glycerol, N′N′N′N′-Tetramethylethylenediamine, Tris base, Tris HCL, sodium chloride, Tween 20 were purchased from Sigma-Aldrich Inc. (St Louis, MO). RNeasy Mini kit, QIA shredder kit, RNeasy Min Elute kit, and Quantitect TM SYBR Green PCR kit were purchased from Qiagen Inc. (Valencia, CA). All primers were purchased from the Iowa State University DNA facility. All primary antibodies were purchased from Abcam (Cambridge, MA) with the exception of the BRCA1(C-20) primary antibody which was from Santa Cruz Biotechnology (Santa Cruz, CA). RNA later was obtained from Ambion Inc. (Austin, TX). Goat antimouse and antirabbit secondary antibodies were obtained from Santa Cruz Biotechnology (Santa Cruz, CA). Ponceau S was from Fisher Scientific. ECL plus chemical luminescence detection kit was obtained from GE Healthcare, Amersham (Buckinghamshire, UK).

Animals and tissue collection

Briefly, 4-week-old female wild type normal nonagouti (a/a; designated lean; n = 10) and agouti lethal yellow (KK.Cg-Ay/J; designated obese; n = 10) were purchased from Jackson laboratories (Bar Harbor, ME 002468). All animals were housed in cages under a 12-h light/dark photoperiod with the temperature between 70 and 73°F and humidity approximately 20–30%. The animals were provided with a standard diet (Teklad 2014 global 14% protein rodent maintenance diet) with ad libitum access to food and water until 6, 12, 18 or 24 weeks of age. These animals were part of a previously described project [41]. Tissues were collected when mice were in the proestrus stage of their estrous cycle. All animal experimental procedures were approved by the Iowa State University Animal Care and Use Committee.

In vivo phosphoramide mustard exposure and tissue collection

A separate group of mice aged 15 weeks in both the lean and obese groups were intraperitoneally (i.p) dosed once with SO or PM (95%; 25 mg/kg) (n = 5/group). This dose was chosen based on the literature [11,42]. Mice were euthanized 3 days after the end of dosing in their proestrus phase. Ovary, uterus, liver, and spleen weights were obtained. One ovary from each mouse was fixed in 4% paraformaldehyde, and one ovary was preserved in RNA *later* at –80°C for RNA and protein isolation.

Ovarian histology and follicle counting

Ovaries were serially sectioned (5-μM thickness) and every sixth section was mounted and stained with hematoxylin and eosin. Numbers of healthy follicles were classified and counted in every sixth section according to the procedures as previously described [11].

RNA isolation and quantitative RT-PCR

Total ovarian RNA was isolated using an RNeasy Mini kit (Qiagen) and the concentration was determined using an ND-1000 Spectrophotometer (λ = 260/280 nm; NanoDrop technologies, Inc., Wilmington, DE) (n = 3 per genotype and treatment). Total RNA (200 ng) was reverse transcribed to complementary DNA (cDNA) utilizing the Superscript III One-Step reverse-transcriptase polymerase chain reaction (RT-PCR) (Qiagen). Complementary DNA was diluted (1:20) in RNase-free water. Diluted cDNA (2 μl) was amplified on an Eppendorf PCR Master cycler using Quantitect SYBR Green PCR kit (Qiagen). Primers sequences were: *Atm*: Forward: TCAGCAGCACCTCTGATTCTT, Reverse: AGACA-GACATGCTGCCTCCT; *Brca1:* Forward: CCCTCTTAGTCT-GCTGAGCT, Reverse: CCTTTGGGTGGCTGTACTGA; *Prkdc:* Forward: GCCACAGACCCCAATATCCT, Reverse: TATCT-GACCATCTCGCCAGC; *Parp1:* Forward: AAGTGCCAGT-GTCAAGGAGA, Reverse: ACAGGGAGCAAAAGGGAAGA; *Rad51:* Forward: ATCCCTGCATGCTTGTTCTC, Reverse: CTGCAGCTGACCATAACGAA; *Xrcc6:* Forward GATCTGA-CACTGCCCAAGG, Reverse: TGCTTCTTCGGTCCACTCTT and *Gapdh:* Forward: GGATGGAATTGTGAGGGGAG, Reverse: GTGGACCTCATGGCCTACAT were designed by Primer 3 Input Version (0.4.0) [43]. The regular cycling program consisted of a 15-min hold at 95°C and 45 cycles of denaturing at 95°C for 15 s, annealing at 58°C for 15 s, and extension at 72°C for 20 s at which point data were acquired. There was no difference in *Gapdh* messenger RNA (mRNA) expression between treatments, thus each sample was normalized to *Gapdh* before quantification. Quantification of fold change in gene expression was performed using the $2^{-\Delta\Delta Ct}$ method [44,45].

Protein isolation and Western blotting

Total ovarian protein was isolated by homogenization in tissue lysis buffer containing protease and phosphatase inhibitors as previously described [31]. Briefly, homogenized samples were placed on ice for 30 min, followed by two rounds of centrifugation at 10,000 rpm for 15 min, and protein concentration was measured using a standard bicinchoninic acid (BCA) protocol. sodium dodecyl sulfate polyacrylamide gel electrophoresis (SDS-PAGE) was used to separate protein homogenates (30 μg) from three randomly chosen animals (unbiased sample selection; n = 3 per genotype and treatment) which were then transferred to a nitrocellulose membrane. Membranes were blocked for 1 h in 5% milk in Tris-buffered saline

containing Tween 20, followed by incubation with one of antirabbit PARP1 antibody (Abcam, cat no: ab6079; dilution—1:200), antirabbit phosphorylated H2AX antibody (γH2AX; Abcam, cat no: ab94602; dilution—1:100), antimouse ATM antibody (Abcam, cat no: ab78; dilution—1:100), antimouse RAD51 antibody (Abcam, cat no: ab1837; dilution—1:500), antimouse XRCC6 antibody (Abcam, cat no: ab3108; dilution—1:100), antirabbit BRCA1 antibody (Santa Cruz Biotechnology, cat no: SC-642; dilution—1:500), or antirabbit PRKDC antibody (Abcam, cat no: ab32566; dilution—1:100) for 36 h at 4°C. Following three washes in TTBS (1×), membranes were incubated with species-specific secondary antibodies (1:2000-5000) for 1 h at room temperature. Membranes were washed 3× in TTBS and incubated in enhanced chemiluminescence detection substrate (ECL plus) for 5 min followed by X-ray film exposure. Densitometry of the appropriate bands was performed using ImageJ software (NCBI). Equal protein loading was confirmed by Ponceau S staining of membranes and protein level was normalized to Ponceau S densitometry values.

Statistical analysis

Raw data for all the experiments were analyzed by one-way analysis of variance (ANOVA) and unpaired t-tests using Graphpad Prism 5.04 software. In addition, two-way ANOVA was performed to investigate potential interaction between PM exposure and obesity and positive interaction is noted in specific endpoint descriptions. Different letters indicate *P*-value < 0.05 was considered a significant difference between treatments. In some instances, additional comparisons to indicate statistical difference at $P < 0.05$ are indicated by symbols as indicated in figure legends. For graphical purposes, protein expression is presented as the mean raw densitometry value ±SE of the respective control.

Results

Effect of phosphoramide mustard exposure on body and organ weight in lean and obese female mice

Body weights were obtained prior to PM injection in both the lean and obese groups. As expected, body weight was increased ($P < 0.05$) in mice that were grouped as the obese controls (40.8 ± 0.66 g) and obese PM (43.25 ± 2.28 g) subjects compared to those grouped as lean control (34.0 ± 1.81 g) and lean PM (30.40 ± 1.36 g) (Figure 1A).

Liver weight was increased ($P < 0.05$) in obese control (2.362 ± 0.056 mg) and obese PM (1.960 ± 0.151 mg) compared to lean control (1.290 ± 0.077 mg) and lean PM (1.44 ± 0.084 mg). Phosphoramide mustard exposure reduced liver weight in obese PM (1.960 ± 0.151 mg) compared to obese control (2.362 ± 0.056 mg) mice. An interaction between PM exposure and obesity was noted for liver weight ($P = 0.009$) (Figure 1B).

Spleen weight was increased ($P < 0.05$) in obese (0.142 ± 0.003 mg) compared to lean control subjects (0.123 ± 0.007 mg). Phosphoramide mustard exposure reduced ($P < 0.05$) spleen weight in lean PM (0.095 ± 0.002 mg) compared to lean control (0.123 ± 0.007 mg) mice. Phosphoramide mustard exposure also reduced ($P < 0.05$) spleen weight in obese PM (0.0795 ± 0.002 mg) compared to obese control (0.142 ± 0.003 mg) mice. An interaction between PM exposure and obesity was observed for spleen weight ($P = 0.002$) (Figure 1C).

Ovarian weight was not altered by PM exposure (lean control: 0.0146 ± 0.001 mg; lean PM: 0.0125 ± 0.009 mg). In contrast, PM
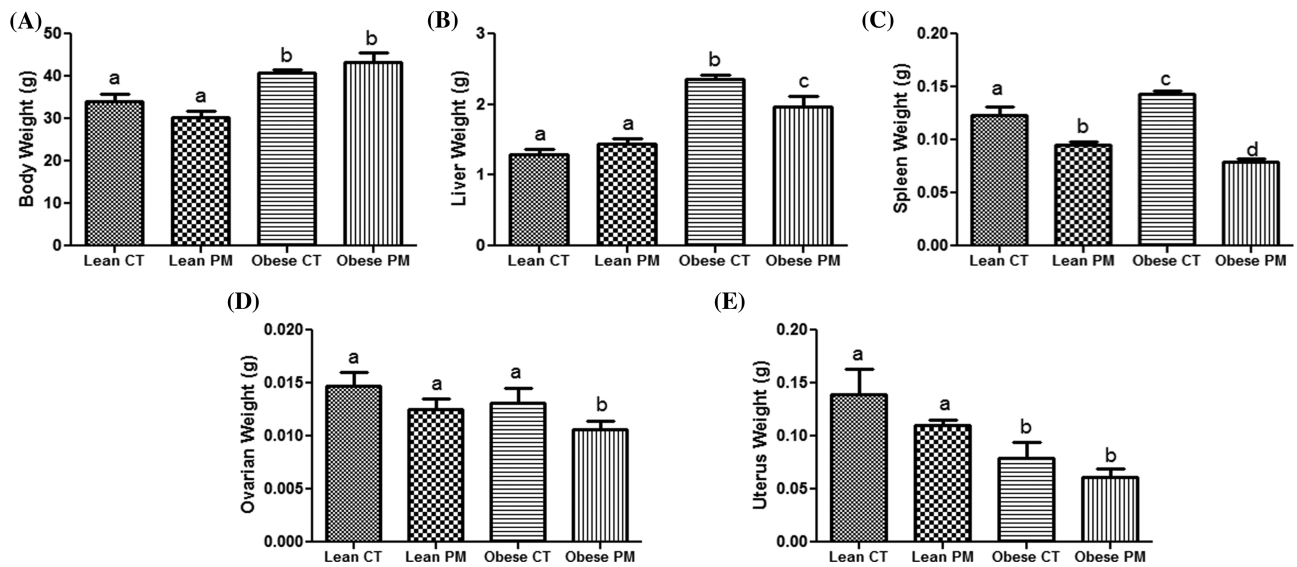
Figure 1. Effect of PM on body and organ weight in lean and obese mice. (A) Body weight was measured at 15 weeks old in both lean and obese group and mice were i.p dosed with SO or PM. (B) Liver, (C) spleen, (D) ovary, and (E) uterus weights were collected posteuthanasia at the proestrus stage of the estrous cycle. Values are expressed as mean ± SE; n = 5. Different letters indicate a statistical difference *P*-value < 0.05.
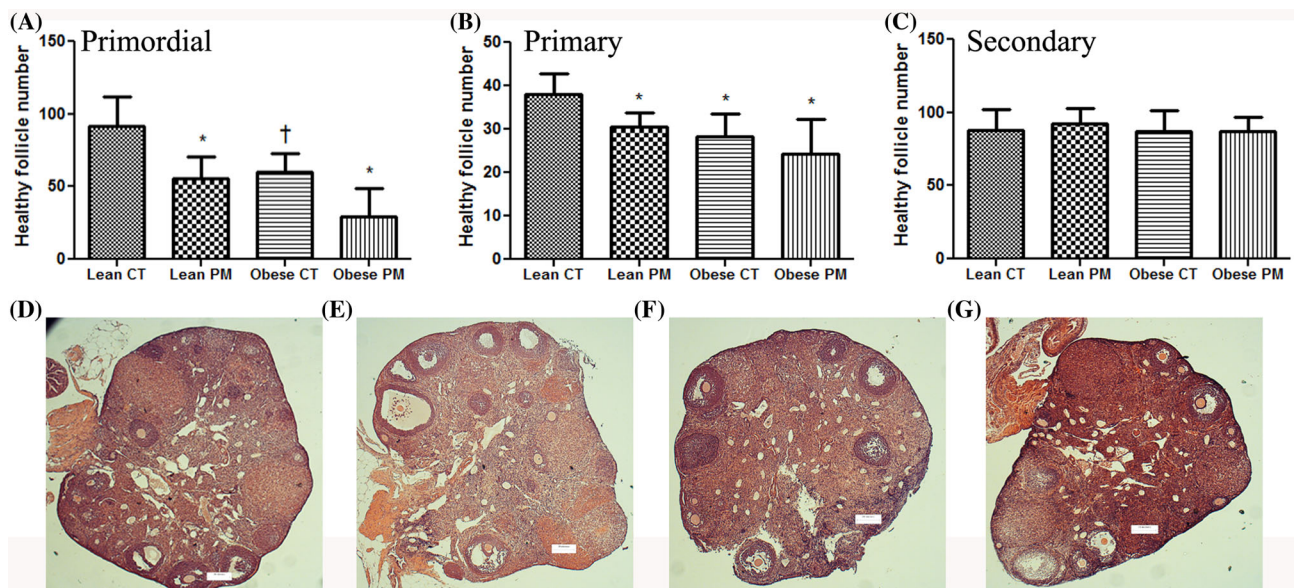

Figure 2. Effect of PM on folliculogenesis in lean and obese mice. Mice were i.p dosed with SO or PM to determine healthy follicles. Follicles are classified as (A) primordial follicles; (B) primary follicles; and (C) secondary follicles. Values are expressed as mean ± SE; n = 5. Statistical significance was defined as *= *P* < 0.05, while *P* < 0.1 was considered a trend towards a difference from control and is indicated with the † symbol. Hematoxylin and eosin-stained ovarian sections were captured at 5× from (D) lean control; (E) lean PM; (F) obese control; and (G) obese PM.

exposure decreased (*P* < 0.05) ovarian weight in obese mice (obese control: 0.0131 ± 0.0013 mg; obese PM: 0.0106 ± 0.0008 mg) relative to their control-treated littermates. As previously reported [40], there were no difference in ovarian weight between lean control and obese control ovaries (Figure 1D).

The uterus weight was decreased (*P* < 0.05) in both the obese control (0.0796 ± 0.014 mg) and obese PM (0.0610 ± 0.007 mg) groups compared to the lean control (0.139 ± 0.024 mg) and lean PM (0.110 ± 0.004 mg) treated mice. There was no effect of PM exposure on uterine weight of lean mice (Figure 1E).

Impact of phosphoramide mustard exposure on folliculogenesis in lean and obese female mice

There were reduced (*P* < 0.07) numbers of healthy primordial follicles in ovaries of obese mice (Lean: CT: 91.4 ± 20.56; Obese: 60.0 ± 12.72) relative to lean controls. Phosphoramide mustard reduced (*P* < 0.05) the number of healthy primordial follicles in both lean (CT: 91.4 ± 20.56; PM: 55.6 ± 15.61) and obese ovaries (CT: 60.0 ± 12.72; PM: 29.5 ± 19.17) compared to lean control (Figure 2A); however, there was no difference in the number of primordial follicles between the obese control and PM-treated groups (Figure 2A).
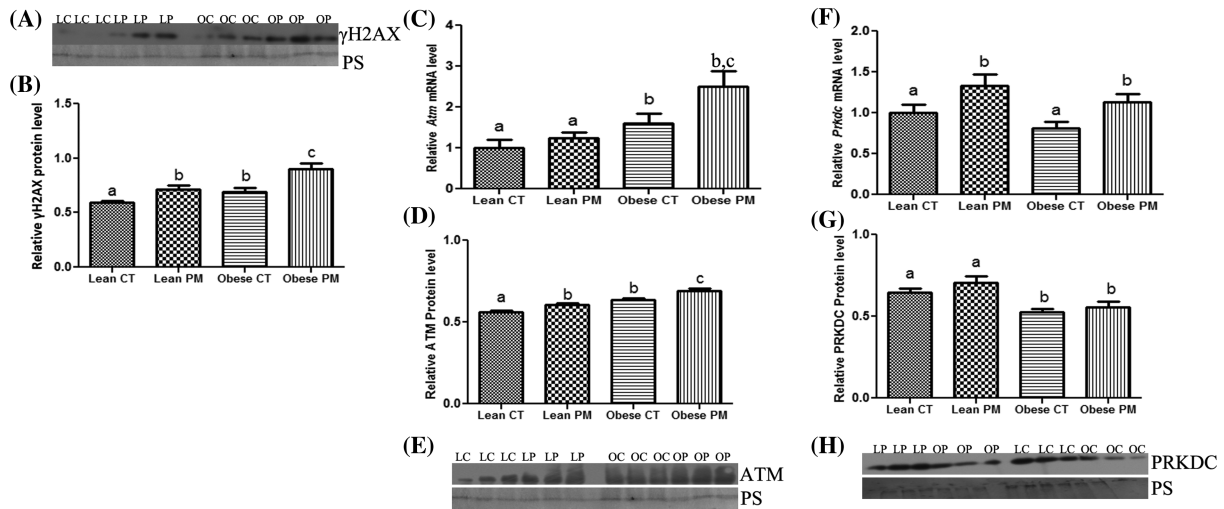
Figure 3. Identification of PM-induced ovarian DNA DSB and induction of the DNA repair response in lean and obese females. Total ovarian RNA or protein were quantified using qPCR or Western blotting, respectively, to determine the effect of PM exposure on the abundance of (A, B) γH2AX protein, (C) *Atm* mRNA, (D, E) ATM protein, (F) *Prkdc* mRNA and (G, H) PRKDC protein in lean and obese ovaries. LC indicates lean control-treated; LP indicates lean PM-treated, OC indicated obese control-treated, and OP indicated obese PM-treated. For qPCR, each sample was normalized to *Gapdh* before quantification. For Western blotting, equal protein loading was confirmed by Ponceau S staining of membranes and protein level was normalized to Ponceau S densitometry values. Values are expressed as mean ± SE; n = 3. Different letters indicate $P < 0.05$.

Identification of phosphoramide mustard-induced DNA double strand breaks and protein markers of DNA repair response induction

The basal level of γH2AX protein was higher ($P < 0.05$) in ovaries from obese (0.69 ± 0.04) compared to lean control mice (0.59 ± 0.01). However, PM exposure increased ($P < 0.05$) γH2AX protein abundance in both lean (CT: 0.59 ± 0.01; PM: 0.71 ± 0.04) and obese (CT: 0.69 ± 0.04; PM: 0.90 ± 0.05) ovaries. There was no interaction between PM exposure and obesity on γH2AX mRNA and protein expression (Figure 3A and B).

Basal levels of *Atm* mRNA were increased ($P < 0.05$) in obese control-treated mice (0.60-fold ± 0.25) compared to lean control ovaries (1.0-fold ± 0.2). While there was no impact of PM exposure in ovaries from lean mice, and increase in *Atm* mRNA was observed in ovaries from obese PM-treated mice (1.5-fold ± 0.39) compared to the vehicle control-treated group (0.60-fold ± 0.25) (Figure 3C). Basal levels of ATM protein were higher ($P < 0.05$) in obese (0.64 ± 0.01) compared to lean vehicle-control-treated ovaries (0.56 ± 0.009). Phosphoramide mustard increased ($P < 0.05$) ATM protein abundance in both the lean (0.60 ± 0.01) and obese PM-exposed ovaries (0.63 ± 0.01). There was no interaction between PM exposure and obesity on ATM mRNA and protein expression (Figure 3D and E).

There were no differences in basal levels of ovarian *Prkdc* mRNA in obese (0.19-fold ± 0.25) compared to lean (1.0-fold ± 0.10) mice. Phosphoramide mustard exposure increased ($P < 0.05$) ovarian *Prkdc* mRNA level in both lean (0.33-fold ± 0.14) and obese (0.32-fold ± 0.10) exposed mice (Figure 3F). PRKDC protein level was lower ($P < 0.05$) in ovaries from obese (CT: 0.52 ± 0.02; PM: 0.56 ± 0.03) compared to lean mice (CT: 0.64 ± 0.02; PM: 0.70 ± 0.03). There was no interaction between PM exposure and obesity on PRKDC mRNA and protein expression (Figure 3G and H).

Basal levels of *Xrcc6* mRNA expression were greatly reduced ($P < 0.05$) in ovaries from obese control (0.70-fold ± 0.05) compared to lean control-treated ovaries (1.0-fold ± 0.13). Phosphoramide mustard decreased ($P < 0.05$) *Xrcc6* mRNA expression in both obese PM (0.78-fold ± 0.02) and lean PM (0.88-fold ± 0.02) ovaries compared to lean control ovaries. An interaction between PM exposure and obesity was noted for *Xrcc6* mRNA abundance ($P = 0.0002$; Figure 4A). Similarly, ovarian XRCC6 protein level was lower ($P < 0.05$) in obese control (0.49 ± 0.02) relative to lean control-treated ovaries (0.65 ± 0.04). Phosphoramide mustard exposure increased ($P < 0.05$) ovarian XRCC6 protein abundance in lean mice (CT: 0.65 ± 0.04; PM: 0.90 ± 0.09), but no impact of PM exposure on XRCC6 protein was observed in obese mice. There was no interaction between PM exposure and obesity on XRCC6 protein expression (Figure 4B and C).

There were no changes in basal levels of *Parp1* mRNA expression in obese control (0.40-fold ± 0.25) compared to lean control (1.0-fold ± 0.10) ovaries. Phosphoramide mustard decreased ($P < 0.05$) *Parp1* mRNA expression in both obese PM (0.82-fold ± 0.02) and lean PM (0.72-fold ± 0.07) treated ovaries compared to the respective control ovaries (Lean: 1.0-fold ± 0.21; Obese 0.40-fold ± 0.18) There was no interaction between PM exposure and obesity on *Parp1* mRNA expression (Figure 4D). There were no changes in basal abundance of total PARP1 protein in obese control (0.69 ± 0.01) compared to lean control (0.69 ± 0.05) ovaries. Phosphoramide mustard increased ($P < 0.05$) total PARP1 protein expression in lean PM ovaries (1.07 ± 0.09) compared to lean control
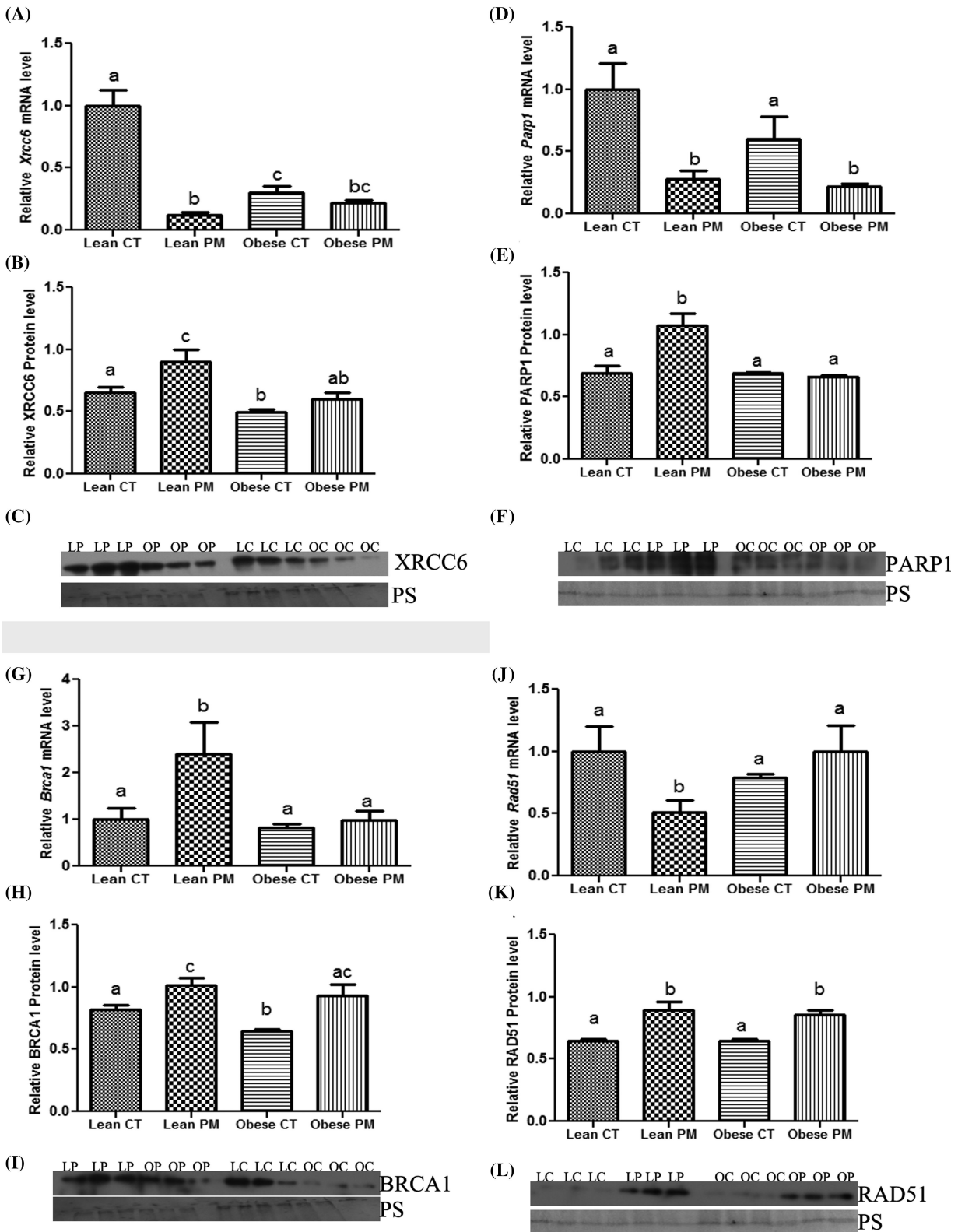
Figure 4. Determination of effect of obesity on PM-induced DNA repair response. Total ovarian RNA or protein were quantified using qPCR or Western blotting, respectively, to determine the effect of PM exposure on the abundance of (A) *Xrcc6* mRNA, (B, C) XRCC6 protein, (D) *Parp1* mRNA, (E, F) PARP1 protein, (G) *Brca1* mRNA, (H, I) BRCA1 protein, (J) *Rad51* mRNA, (K, L) RAD51 protein in lean and obese ovaries. LC indicates lean control-treated; LP indicates lean PM-treated, OC indicated obese control-treated, and OP indicated obese PM-treated. For qPCR, each sample was normalized to *Gapdh* before quantification. For Western blotting, equal protein loading was confirmed by Ponceau S staining of membranes and protein level was normalized to Ponceau S densitometry values. Values are expressed as mean ± SE; n = 3. Different letters indicate *P* < 0.05.
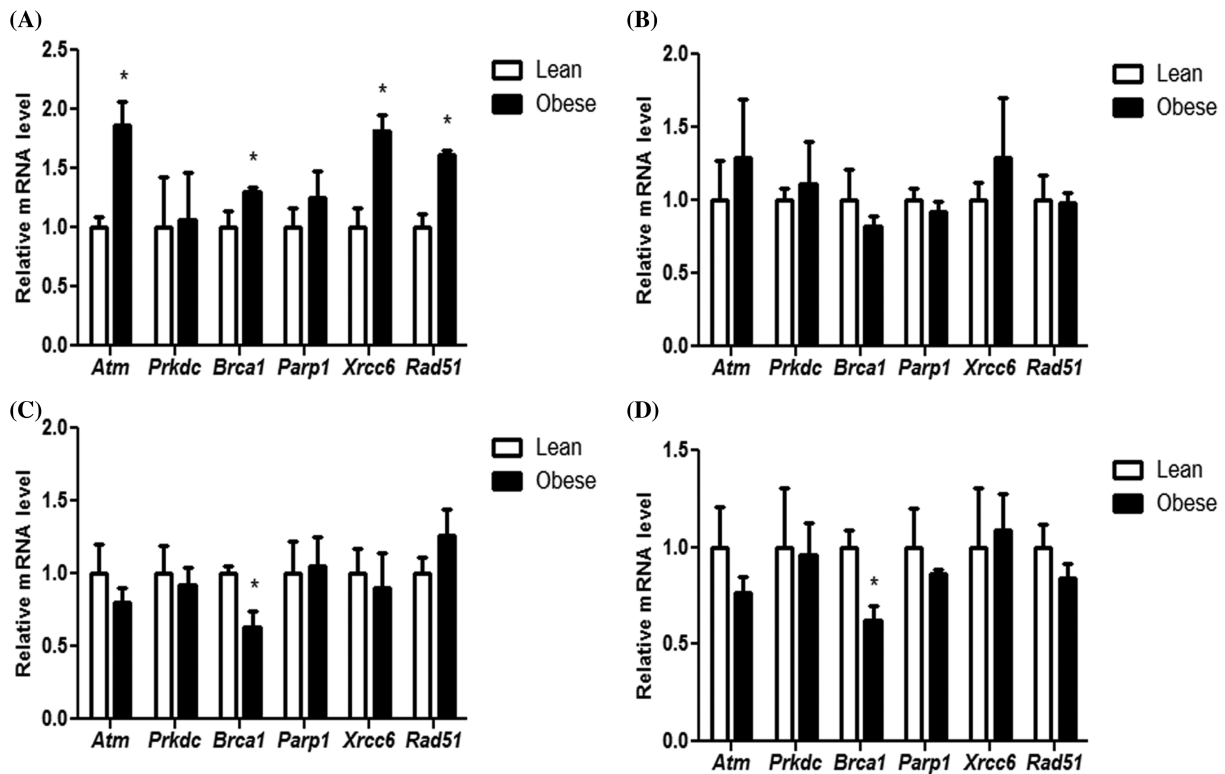
Figure 5. Identification of impact of genotype and obesity progression on expression of genes involved in DNA repair response. Ovaries were collected from (A) 6, (B) 12, (C) 18, or (D) 24-week-old female mice and ovarian total RNA was isolated to perform qRT-PCR. Values are expressed as mean fold change ± SE; n = 3. Statistical significance was defined as $*$ = $P < 0.05$.

(0.69 ± 0.05) ovaries, but there were no changes in total PARP1 protein expression due to PM exposure in ovaries from obese mice. An interaction between PM exposure and obesity for PARP1 protein abundance was noted ($P = 0.006$; Figure 4E and F).

There were no differences in basal level of *Brca1* mRNA expression between the lean and obese ovaries. Phosphoramide mustard increased ($P < 0.05$) *Brca1* mRNA expression in lean PM ovaries (1.4-fold ± 0.68) relative to lean control ovaries, and this increase was absent in ovaries from obese mice (Figure 4G). The basal level of ovarian BRCA1 protein was lower ($P < 0.05$) in obese (0.64 ± 0.01) relative to lean control-treated (0.81 ± 0.03) mice. Phosphoramide mustard increased ($P < 0.05$) BRCA1 protein level in both lean (1.01 ± 0.05) and obese (0.93 ± 0.08) PM-exposed groups compared to their respective controls (Lean: 0.81 ± 0.03; Obese: 0.64 ± 0.01). There was no interaction between PM exposure and obesity on BRCA1 mRNA and protein expression (Figure 4H and I).

Rad51 mRNA expression was not different in obese ovaries compared to lean ovaries. However, PM exposure decreased ($P < 0.05$) ovarian *Rad51* mRNA expression in lean mice (CT: 1.0-fold ± 0.2; PM: 0.49-fold ± 0.10). In contrast, *Rad51* mRNA expression was increased ($P < 0.05$) in response to PM exposure in ovaries from obese mice (1.0-fold ± 0.21) compared to lean mice (0.49-fold ± 0.10). An interaction between PM exposure and obesity for *Rad51* mRNA existed ($P = 0.04$) (Figure 4J). There was no basal differential RAD51 protein abundance in obese compared to lean ovaries. Phosphoramide mustard increased ($P < 0.05$) RAD51 protein level in both lean (0.89 ± 0.06) and obese (0.86 ± 0.03) exposed groups

compared to their respective controls (Lean: 0.65 ± 0.01; Obese: 0.65 ± 0.01). There was no interaction between PM exposure and obesity on RAD51 protein level (Figure 4K and L).

Temporal effect of genotype on DNA repair gene abundance

Since low levels of DNA damage were observed previously [40] and as indicated by increased ϒH2AX protein in this study, the impact of progressive obesity on induction of the DNA repair response was determined. After 6 weeks of age, obese ovaries had increased ($P < 0.05$) expression of a number of DNA DSB repair genes investigated (*Atm*: 0.87 fold ± 0.2; *Brca1*: 0.30 fold ± 0.04; *Xrcc6*: 0.82 fold ± 0.13; *Rad51*: 0.62 fold ± 0.03), compared to the lean mouse strain (Figure 5A).

After 12 weeks of age, there was no differential expression in any of the DNA DSB repair gene between the mouse strains. In the mice aged 18 and 24 weeks of age, *Brca1* mRNA abundance was reduced ($P < 0.05$) in ovaries from obese mice (18 weeks: 0.37 fold ± 0.11; 24 weeks: 0.38 fold ± 0.08) relative to lean mice ovaries (Figure 5B–D).

Discussion

This study investigated PM-induced DNA DSB as an initiating event in follicular atresia. We have previously noted that PM activates the DNA DSB repair mechanism in cultured neonatal rat ovaries [15] and in a rat ovarian granulosa cell line [14], which we propose is a logical mechanism to protect cells from PM-induced ovotoxicity.

Also, obesity induces DNA damage in hematopoietic cells after CPA exposure [25], and we have previously demonstrated that progressive obesity induces DNA damage in ovaries [43]. Thus, the primary objective of this study was to investigate the impact of PM exposure on the DDR in vivo, and secondly to determine any additive impact of obesity on the ovarian protective response to PM exposure.

Obesity increased liver weight which was consistent with another study in which a high-fat diet increased liver weights in male wistar rats [46,47]. Obesity increased spleen weight in this study, as previously observed in high-fat-diet-fed mice [47]. No major effect of PM on organ weights was observed in the absence of obesity, with the exception of spleen weight which was reduced in both the lean and obese mice. However, we did not note an interaction between PM exposure and obesity in both liver and spleen weights. A single exposure of CPA (250 mg/kg) was found to increase liver weight after 8 days in CD-1 female mice [13]. In that study, spleen weights were decreased 1 day after exposure, similar to our findings, but were increased 8 days later in mice dosed with 150 or 250 mg/kg CPA [13]. We found that ovarian weight was not altered by obesity at the time point chosen, similar to our previously published findings [40] while uteri was reduced in weight. We discovered that a single dose of PM decreased ovarian weight in obese mice, consistent with a previous study that in utero exposure of CPA reduced ovarian weight in mice [48]. Taken together, PM reduced ovary and spleen weights while obesity altered uterus, spleen, and liver weights. Whether increased hepatic weight was due to fatty liver was not determined in this study but could potentially impact biotransformation and detoxification of PM (and other chemicals) and is an area for future consideration.

Phosphoramide mustard is a known ovotoxicant and destroys primordial and primary follicles in mice and rat ovaries both in in vitro and ex vivo models [12,15,49,50] and in vivo [8,51]. A single PM dose reduced primordial and primary follicles in lean mice. There was a lower number of primordial and primary follicles numbers in obese mouse ovaries, but, surprisingly, no additive effect of PM in obese ovaries and no interaction between PM exposure and obesity was observed. The numbers of secondary follicles were not changed by lean and obese PM, potentially indicating that smaller follicles are more sensitive to PM-induced ovotoxicity than larger follicles. However, our in vitro PM exposure studies demonstrated reductions in all follicular types compared to control which might be attributable to direct ovarian exposure in those studies [12,15]. The lower number of follicles due to obesity was in agreement with a previous study from our group which demonstrated that obesity reduced primordial and primary follicle number after 12 weeks of age [41]. Since maintenance of primordial follicles in a dormant but viable state is essential for normal reproductive activity, reduction of primordial follicle pool can lead to premature ovarian failure [1]. Interestingly, reduced ovarian weight was noted in obese mice exposed to PM, which is not explained by fewer numbers of ovarian follicles relative to the control-treated obese mice. We counted healthy follicles since we have recently determined that PM induces autophagy markers in exposed ovaries, and we have noted that unhealthy follicles are rapidly removed from the ovary postatresia [52]

Localization of γH2AX protein is considered a gold standard technique for identification of DNA DSB [53] and PM exposure increased γH2AX protein in both lean and obese mice. Thus, these data corroborate our in vitro data and demonstrate that PM-induced ovotoxicity involves the formation of DNA DSB. We have previously reported [43], and again demonstrate herein that obesity results in low-level DNA DSBs as evidenced by the presence of ovarian γH2AX. We do not know the cause of such DNA DSB in ovaries

from obese mice, but speculate that increased reactive oxygen species could be present [54]. Considering that protection of the germline is an evolutionary necessity, we next investigated that ovarian capacity for DNA DSB repair.

Ataxia-telangiectasia mutated is a protein kinase which activates downstream signaling molecules that involved in the DNA repair process. Ataxia-telangiectasia mutated phosphorylates P53 to initiate cell cycle arrest [55], DNA repair genes [56] and to regulate the expression of apoptosis-related genes [57]. Phosphoramide mustard exposure resulted in increased *Atm* mRNA and/or protein abundance in both lean and obese ovaries, confirming that DNA DSB formation is a result of ovarian PM exposure. We have previously shown the same effect in two in vitro models; cultured granulosa cells [14] and cultured neonatal ovaries [15], thus these data confirm that ATM activation is an ovarian event that results from PM exposure. Interestingly, *Atm* mRNA was higher in ovaries from obese compared to lean mice. These data indicate that ATM acts as an ovarian sensor of DNA DSBs and activates DNA repair mechanism and that obesity did not impact that aspect of the ovarian DNA repair response. Ataxia-telangiectasia mutated's involvement as a sensor of ovotoxicity and a potential coordinator of the ovarian response to DNA-damaging events is further supported by our work with both DMBA [43,58] and bisphenol A [59].

A protein that involved in the NHEJ repair pathway is PRKDC, a DNA-dependent protein kinase which activates P53 through coordination with CHK2 [60]. *Prkdc* gene expression was increased by PM exposure in both lean and obese ovaries indicating that the NHEJ repair pathway was being activated in PM-exposed ovaries. We have previously found the same effect in cultured granulosa cells [14] and neonatal cultured rat ovaries [15] after PM exposure. Interestingly, PRKDC protein was at a lower level in ovaries from obese mice and no increase in PRKDC protein level after PM exposure was observed in those mice, which was similar to another study from our group which investigated the impact of DMBA exposure in lean and obese mice [43]. Inhibition of PRKDC enhances heat-induced apoptosis independent of heat shock protein in human cervical carcinoma HeLa S3 cells [61]. These data indicate obesity has lower basal abundance of PRKDC protein abundance which could impact the ovarian capacity for DNA repair.

XRCC6 is a KU protein essential for formation of heterodimer with XRCC5 and is also part of the NHEJ repair pathway. Ovarian XRCC6 protein was increased by PM exposure in lean mice but this response was absent in obese females. This lowered PRKDC response might be potentially due to basal DNA damage which is present in ovarian tissue during obesity. We have previously found that PM increased XRCC6 protein expression in spontaneously immortalized granulosa cells (SIGC) cells [14], while progressive obesity resulted in decreased XRCC6 protein expression [43]. Decreased XRCC6 representing defective DNA repair and chromosomal instability has been reported in embryonic cells [62]. Thus, PM may activate DNA repair via XRCC6 but obesity attenuates this molecular event, thus compromising DNA repair.

PARP1 regulates DNA repair and cell survival [63–65]. Phosphoramide mustard exposure decreased *Parp1* mRNA expression irrespective of metabolic status, while total PARP1 protein was increased only in lean ovaries. Our previous study from SIGC cells found that PM increased total PARP1 protein abundance regardless of dose and time of exposure [14] and in rat neonatal cultured ovaries [15]. There were no changes in total PARP1 protein level while PM decreased mRNA expression in obese ovaries. In the absence of PARP1, when DNA breaks are encountered during DNA

Table 1. Antibodies used in this study.

Protein target	Supplier	Catalogue Number	Dilution
BRCA1	Santa Cruz Biotechnology	sc-642	1:500
PARP1	Abcam	ab6079	1:200
γH2AX	Abcam	ab94602	1:100
ATM	Abcam	ab78	1:100
RAD51	Abcam	ab1837	1:500
XRCC6	Abcam	ab3108	1:100
PRKDC	Abcam	ab32566	1:100

replication, the replication fork stalls, and DSBs accumulated in synchronized HeLa cells by radiation exposure [66]. These data suggest that absence of increased PARP1 protein in response to PM during obesity may contribute to increased DNA damage in obese ovaries, whether this is due to altered translation of Parp1 mRNA to protein remains unclear and for future consideration.

BRCA1 repairs DNA DSBs through the HR pathway. Impairment of BRCA1-related DNA DSB repair has been associated with accelerated loss of the ovarian follicular reserve and with accumulation of DSB in human oocytes, suggesting that DNA DSB repair efficiency is an important determinant of oocyte aging in women [28]. Phosphoramide mustard increased *Brca1* mRNA and protein expression, while BRCA1 protein was itself basally lowered by obesity. This is consistent with our data demonstrating that PM increased BRCA1 protein abundance in cultured neonatal rat ovaries [15] and progressive obesity reduced ovarian BRCA1 protein [43]. The data from this study suggest that BRCA1 is induced as part of the ovarian protective response to PM exposure and the HR pathway is activated. In addition, reduction of BRCA1 by obesity may accelerate ovarian follicle loss and aging by reducing DNA repair.

RAD51 plays a major role in HR repair using sister chromatids and was increased by PM exposure in both lean and obese ovaries, while mRNA abundance was decreased by PM exposure in lean ovaries. RAD51 interacts with BRCA1 during the DDR, and DMBA exposure increased RAD51 protein abundance in both prostate tissue [67] and in SIGC cells in a dose- and time-dependent manner [58]. Also, RAD51 protein level was reduced at the time of follicle loss in neonatal cultured rat ovaries after PM exposure [15]. The RAD51 protein response to PM exposure was consistent with the pattern of BRCA1 expression post-PM exposure.

Taken together, these data described herein strongly support that PM induces DNA DSBs to which the ovary responds by activation of the DDR. Of concern is that a blunted ovarian DDR was observed in obese mice, potentially contributory to the basal DNA DSB apparent in these ovaries. Since a blunted DDR was supported by the data from obese ovarian tissue, we examined basal mRNA abundance of DDR genes during progressive obesity from samples available through another study by our group. *Atm*, *Brca1*, *Xrcc6,* and *Rad51* mRNA abundance were increased due to obesity at 6 weeks of age, but no other changes with the exception of reduced *Brca1* were noted at other time points examined. This seems paradoxical since ΥH2AX was observed in the absence of a chemical insult in ovaries from obese mice. It should be noted that this study only examined one time point of PM exposure, and perhaps the DDR occurred at a faster rate in ovaries from obese ovaries than those from lean mice; however, the occurrence of ΥH2AX in obese ovarian tissue does not support this theory, since an altered, more rapid DDR should remove any DNA damage occurring in the cell.

A recent study by our group determined that pharmaceutical inhibition of ATM using KU55933 completely prevented PM-induced loss of primordial follicles and partially prevented primary follicle loss [15], a phenotype reminiscent of that observed in this study in the obese mice exposure to PM, who did not suffer follicle loss when compared to their respective controls. Could compromised ATM function be culpable for such a phenotype? We consider this a possibility since proteins downstream of ATM have altered capacity to respond to PM exposure in the obese mice. Thus, investigating the kinase activity of ATM is a current area that we are pursuing. As noted earlier, we have observed markers of autophagy to be increased post-PM exposure in cultured whole ovaries [52] and have determined that PM induces classic apoptotic markers, including cleaved caspase 3, P73, and E2F7 [14,15], thus in the absence of pharmaceutical intervention, atresia due to PM exposure eventually occurs; however, it is likely that ATM coordinates halting of the cell cycle for DNA repair to proceed, and if such repair is insufficient, the follicle is shunted towards an atretic fate. In the absence of ATM function, follicles may remain, as in the case of ATM inhibition pharmaceutically, but may have compromised oocyte quality. This is a research question which we are actively investigating.

In conclusion, PM-induced ovarian DNA damage in vivo with an accompanying increase in the ovarian protective response to counteract such damage. Obesity altered the ovarian response to PM exposure, and whether this could contribute to a poorer reproductive outcome following CPA/PM treatment remains unclear, but is worthy of consideration. Since we found an interaction between PM exposure and obesity in liver weight, we propose that hepatic xenobiotic metabolism might be affected by obesity which could contribute to ovotoxicity induced by PM. In some cases, a disconnect between mRNA and protein induction was noted in this study, which may shed light on feedback loops that are important for coordination of the ovarian DDR and serve as candidates for investigation into this area. Future work directed at preventing PM-induced ovarian DNA damage remains necessary and to further clarify the impact of altered physiological status on chemotherapeutic outcomes. Additionally, investigation of localization and cellular compartment within the ovary in which changes to these proteins of interest are altered is vital for these studies. Furthermore, determining the temporal pattern of obesity onset on ovotoxicity as well as determining if the data generated in this study extend to models which use high-fat diets to induce obesity are warranted.

References

1. Hirshfield AN. Development of follicles in the mammalian ovary. *Int Rev Cytol* 1991; **124**:43–101.
2. Fortune JE, Cushman RA, Wahl CM, Kito S. The primordial to primary follicle transition. *Mol Cell Endocrinol* 2000; **163**:53–60.
3. Hoyer PB, Sipes IG. Assessment of follicle destruction in chemical-induced ovarian toxicity. *Ann Rev Pharm Toxicol* 1996; **36**:307–331.
4. Pal L, Santoro N. Premature ovarian failure (POF): discordance between somatic and reproductive aging. *Ageing Res Rev* 2002; **1**:413–423.
5. Brunner HI, Bishnoi A, Barron AC, Houk LJ, Ware A, Farhey Y, Mongey AB, Strife CF, Graham TB, Passo MH. Disease outcomes and ovarian function of childhood-onset systemic lupus erythematosus. *Lupus* 2006; **15**:198–206.
6. Kalich-Philosoph L, Roness H, Carmely A, Fishel-Bartal M, Ligumsky H, Paglin S, Wolf I, Kanety H, Sredni B, Meirow D. Cyclophosphamide triggers follicle activation and "burnout"; as101 prevents follicle loss and preserves fertility. *Sci Trans Med* 2013; **5**:185ra162.

7. Keating AF, Mark CJ, Sen N, Sipes IG, Hoyer PB. Effect of phosphatidylinositol-3 kinase inhibition on ovotoxicity caused by 4-vinylcyclohexene diepoxide and 7, 12-dimethylbenz[a]anthracene in neonatal rat ovaries. *Toxicol Appl Pharmacol* 2009; **241**:127–134.

8. Plowchalk DR, Mattison DR. Phosphoramide mustard is responsible for the ovarian toxicity of cyclophosphamide. *Toxicol Appl Pharmacol* 1991; **107**:472–481.

9. Jarrell JF, Bodo L, YoungLai EV, Barr RD, O'Connell GJ. The short-term reproductive toxicity of cyclophosphamide in the female rat. *Reprod Toxicol* 1991; **5**:481–485.

10. Ludeman SM. The chemistry of the metabolites of cyclophosphamide. *Curr Pharm Des* 1999; **5**:627–643.

11. Desmeules P, Devine PJ. Characterizing the ovotoxicity of cyclophosphamide metabolites on cultured mouse ovaries. *Toxicol Sci* 2006; **90**:500–509.

12. Madden JA, Hoyer PB, Devine PJ, Keating AF. Involvement of a volatile metabolite during phosphoramide mustard-induced ovotoxicity. *Toxicol Appl Pharmacol* 2014; **277**:1–7.

13. Petrillo SK, Desmeules P, Truong T-Q, Devine PJ. Detection of DNA damage in oocytes of small ovarian follicles following phosphoramide mustard exposures of cultured rodent ovaries in vitro. *Toxicol Appl Pharmacol* 2011; **253**:94–102.

14. Ganesan S, Keating AF. Phosphoramide mustard exposure induces DNA adduct formation and the DNA damage repair response in rat ovarian granulosa cells. *Toxicol Appl Pharmacol* 2015; **282**: 252–258.

15. Ganesan S, Keating AF. The ovarian DNA damage repair response is induced prior to phosphoramide mustard-induced follicle depletion, and ataxia telangiectasia mutated inhibition prevents PM-induced follicle depletion. *Toxicol Appl Pharmacol* 2016; **292**:65–74.

16. Surya YA, Rosenfeld JM, Hillcoat BL. Cross-linking of DNA in L1210 cells and nuclei treated with cyclophosphamide and phosphoramide mustard. *Cancer Treat Rep* 1978; **62**:23–29.

17. Murnane JP, Byfield JE. Irreparable DNA cross-links and mammalian cell lethality with bifunctional alkylating agents. *Chem Biol Interact* 1981; **38**:75–86.

18. Chetsanga CJ, Polidori G, Mainwaring M. Analysis and excision of ring-opened phosphoramide mustard-deoxyguanine adducts in DNA. *Cancer Res* 1982; **42**:2616–2621.

19. Giunta S, Belotserkovskaya R, Jackson SP. DNA damage signaling in response to double-strand breaks during mitosis. *J Cell Biol* 2010; **190**:197–207.

20. Elkind MM, Moses WB, Sutton-Gilbert H. Radiation response of mammalian cells grown in culture. VI. Protein, DNA, and RNA inhibition during the repair of x-ray damage. *Radiat Res* 1967; **31**:156–173.

21. Gaudin D, Gregg RS, Yielding KL. Inhibition of DNA repair replication by DNA binding drugs which sensitize cells to alkylating agents and X-rays. *Proc Soc Exp Biol Med* 1972; **141**:543–547.

22. Valeriote F, van Putten L. Proliferation-dependent cytotoxicity of anticancer agents: a review. *Cancer Res* 1975; **35**:2619–2630.

23. Meirow D, Epstein M, Lewis H, Nugent D, Gosden RG. Administration of cyclophosphamide at different stages of follicular maturation in mice: effects on reproductive performance and fetal malformations. *Hum Reprod* 2001; **16**:632–637.

24. Byrne J, Rasmussen SA, Steinhorn SC, Connelly RR, Myers MH, Lynch CF, Flannery J, Austin DF, Holmes FF, Holmes GE, Strong LC, Mulvihill JJ. Genetic disease in offspring of long-term survivors of childhood and adolescent cancer. *Am J Hum Genet* 1998; **62**:45–52.

25. Johnson LA, Tretyakova N, Jacobson PA. Obesity effects on cyclophosphamide-induced DNA damage in hematopoietic cell transplant recipients. *In Vivo* 2012; **26**:853–857.

26. Gandhi, G, Kaur, G. Assessment of DNA damage in obese individuals. *Res J Biol* 2012; **2**:37–44.

27. Djuric Z, Kritchevsky D. Modulation of oxidative DNA damage levels by dietary fat and calories. *Mut Res* 1993; **295**:181–190.

28. Titus S, Li F, Stobezki R, Akula K, Unsal E, Jeong K, Dickler M, Robson M, Moy F, Goswami S, Oktay K. Impairment of BRCA1-related DNA double-strand break repair leads to ovarian aging in mice and humans. *Sci Trans Med* 2013; **5**:172ra121.

29. Brewer CJ, Balen AH. The adverse effects of obesity on conception and implantation. *Reproduction* 2010; **140**:347–364.

30. Kulie T, Slattengren A, Redmer J, Counts H, Eglash A, Schrager S. Obesity and women's health: an evidence-based review. *J Am Board Fam Med* 2011; **24**:75–85.

31. Zaadstra BM, Seidell JC, Van Noord PA, te Velde ER, Habbema JD, Vrieswijk B, Karbaat J. Fat and female fecundity: prospective study of effect of body fat distribution on conception rates. *BMJ* 1993; **306**:484–487.

32. Crosignani PG, Ragni G, Parazzini F, Wyssling H, Lombroso G, Perotti L. Anthropometric indicators and response to gonadotrophin for ovulation induction. *Hum Reprod* 1994; **9**:420–423.

33. Rachoń D, Teede H. Ovarian function and obesity—interrelationship, impact on women's reproductive lifespan and treatment options. *Mol Cell Endocrinol* 2010; **316**:172–179.

34. Rich-Edwards JW, Goldman MB, Willett WC, Hunter DJ, Stampfer MJ, Colditz GA, Manson JE. Adolescent body mass index and infertility caused by ovulatory disorder. *Am J Obstet Gynecol* 1994; **171**:171–177.

35. Owens LA, Avalos G, Kirwan B, Carmody L, Dunne F. ATLANTIC DIP: closing the loop: a change in clinical practice can improve outcomes for women with pregestational diabetes. *Diabetes Care* 2012; **35**:1669–1671.

36. Purcell SH, Moley KH. The impact of obesity on egg quality. *J Assist Reprod Genet* 2011; **28**:517–524.

37. Benedetto C, Salvagno F, Canuto EM, Gennarelli G. Obesity and female malignancies. *Best Pract Res Clin Obstet Gynaecol* 2015; **29**:528–540.

38. Nagle CM, Dixon SC, Jensen A, Kjaer SK, Modugno F, deFazio A, Fereday S, Hung J, Johnatty SE, Fasching PA, Beckmann MW, Australian Ovarian Cancer Study G et al. Obesity and survival among women with ovarian cancer: results from the Ovarian Cancer Association Consortium. *Br J Cancer* 2015; **113**:817–826.

39. Eriksson JG, Sandboge S, Salonen MK, Kajantie E, Osmond C. Long-term consequences of maternal overweight in pregnancy on offspring later health: findings from the Helsinki Birth Cohort Study. *Ann Med* 2014; **46**:434–438.

40. Nteeba J, Ganesan S, Keating AF. Impact of obesity on ovotoxicity Induced by 7,12-dimethylbenz[a]anthracene in mice. *Biol Reprod* 2014; **90**:68, 61–10.

41. Nteeba J, Ganesan S, Keating AF. Progressive obesity alters ovarian folliculogenesis with impacts on pro-inflammatory and steroidogenic signaling in female mice. *Biol Reprod* 2014; **91**:86.

42. Mattison DR, Nightingale MS, Shiromizu K. Effects of toxic substances on female reproduction. *Environ Health Perspect* 1983; **48**:43–52.

43. Ganesan S, Nteeba J, Keating AF. Enhanced susceptibility of ovaries from obese mice to 7,12-dimethylbenz[a]anthracene-induced DNA damage. *Toxicol Appl Pharmacol* 2014; **281**:203–210.

44. Livak KJ, Schmittgen TD. Analysis of relative gene expression data using real-time quantitative PCR and the 2−ΔΔCT method. *Methods* 2001; **25**:402–408.

45. Pfaffl MW. A new mathematical model for relative quantification in real-time RT-PCR. *Nucleic Acids Res* 2001; **29**:e45.

46. Milagro FI, Campión J, Martínez JA. Weight gain induced by high-fat feeding involves increased liver oxidative stress. *Obesity* 2006; **14**:1118–1123.

47. DeLany JP, Blohm F, Truett AA, Scimeca JA, West DB. Conjugated linoleic acid rapidly reduces body fat content in mice without affecting energy intake. *Am J Physiol* 1999; **276**:R1172–R1179.

48. Comish PB, Drumond AL, Kinnell HL, Anderson RA, Matin A, Meistrich ML, Shetty G. Fetal cyclophosphamide exposure induces testicular cancer and reduced spermatogenesis and ovarian follicle numbers in mice. *PLoS One* 2014; **9**:e93311.

49. Madden JA, Keating AF. Ovarian xenobiotic biotransformation enzymes are altered during phosphoramide mustard-induced ovotoxicity. *Toxicol Sci* 2014; **141**:441–452.

50. Petrillo SK, Desmeules P, Truong TQ, Devine PJ. Detection of DNA damage in oocytes of small ovarian follicles following phosphoramide mustard

exposures of cultured rodent ovaries in vitro. *Toxicol Appl Pharmacol* 2011; **253**:94–102.

51. Plowchalk DR, Mattison DR. Reproductive toxicity of cyclophosphamide in the C57BL/6N mouse: 1. Effects on ovarian structure and function. *Reprod Toxicol* 1992; **6**:411–421.

52. Madden JA, Thomas PQ, Keating AF. Phosphoramide mustard induces autophagy markers and mTOR inhibition prevents follicle loss due to phosphoramide mustard exposure. *Reprod Toxicol* 2016; **67**:65–78.

53. Paull TT, Rogakou EP, Yamazaki V, Kirchgessner CU, Gellert M, Bonner WM. A critical role for histone H2AX in recruitment of repair factors to nuclear foci after DNA damage. *Curr Biol* 2000; **10**:886–895.

54. Igosheva N, Abramov AY, Poston L, Eckert JJ, Fleming TP, Duchen MR, McConnell J. Maternal diet-induced obesity alters mitochondrial activity and redox status in mouse oocytes and zygotes. *PLoS One* 2010; **5**:e10074.

55. Zhou B-BS, Elledge SJ. The DNA damage response: putting checkpoints in perspective. *Nature* 2000; **408**:433–439.

56. Starita LM, Parvin JD. The multiple nuclear functions of BRCA1: transcription, ubiquitination and DNA repair. *Curr Opin Cell Biol* 2003; **15**:345–350.

57. Banin S, Moyal L, Shieh S-Y, Taya Y, Anderson CW, Chessa L, Smorodinsky NI, Prives C, Reiss Y, Shiloh Y, Ziv Y. Enhanced phosphorylation of p53 by ATM in response to DNA damage. *Science* 1998; **281**:1674–1677.

58. Ganesan S, Bhattacharya P, Keating AF. 7,12-Dimethylbenz[a]anthracene exposure induces the DNA repair response in neonatal rat ovaries. *Toxicol Appl Pharmacol* 2013; **272**:690–696.

59. Ganesan S, Keating AF. Bisphenol A-induced ovotoxicity involves DNA damage induction to which the ovary mounts a protective response indicated by increased expression of proteins involved in DNA repair and xenobiotic biotransformation. *Toxicol Sci* 2016; **152**:169–180.

60. Jack MT, Woo RA, Motoyama N, Takai H, Lee PWK. DNA-dependent protein kinase and checkpoint kinase 2 synergistically activate a latent population of p53 upon DNA damage. *J Biol Chem* 2004; **279**:15269–15273.

61. Okazawa S, Furusawa Y, Kariya A, Hassan MA, Arai M, Hayashi R, Tabuchi Y, Kondo T, Tobe K. Inactivation of DNA-dependent protein kinase promotes heat-induced apoptosis independently of heat-shock protein induction in human cancer cell lines. *PLoS One* 2013; **8**:e58325.

62. Gu Y, Jin S, Gao Y, Weaver DT, Alt FW. Ku70-deficient embryonic stem cells have increased ionizing radiosensitivity, defective DNA end-binding activity, and inability to support V(D)J recombination. *Proc Natl Acad USA* 1997; **94**:8076–8081.

63. Wang Z-Q, Stingl L, Morrison C, Jantsch M, Los M, Schulze-Osthoff K, Wagner EF. PARP is important for genomic stability but dispensable in apoptosis. *Genes Dev* 1997; **11**:2347–2358.

64. Ziegler M, Oei SL. A cellular survival switch: poly(ADP-ribosyl)ation stimulates DNA repair and silences transcription. *Bioessays* 2001; **23**:543–548.

65. Satoh MS, Lindahl T. Role of poly(ADP-ribose) formation in DNA repair. *Nature* 1992; **356**:356–358.

66. Noël G, Godon C, Fernet M, Giocanti N, Mégnin-Chanet F, Favaudon V. Radiosensitization by the poly(ADP-ribose) polymerase inhibitor 4-amino-1,8-naphthalimide is specific of the S phase of the cell cycle and involves arrest of DNA synthesis. *Mol Cancer Ther* 2006; **5**:564–574.

67. Xu J, Osuga Y, Yano T, Morita Y, Tang X, Fujiwara T, Takai Y, Matsumi H, Koga K, Taketani Y, Tsutsumi O. Bisphenol A induces apoptosis and G2-to-M arrest of ovarian granulosa cells. *Biochem Biophys Res Comm* 2002; **292**:456–462.